Development 134, 3317-3326 (2007) doi:10.1242/dev.02883

Vascular remodeling of the mouse yolk sac requires hemodynamic force

Jennifer L. Lucitti[1,*], Elizabeth A. V. Jones[2,*], Chengqun Huang[3], Ju Chen[3], Scott E. Fraser[4] and Mary E. Dickinson[1,4,†]

The embryonic heart and vessels are dynamic and form and remodel while functional. Much has been learned about the genetic mechanisms underlying the development of the cardiovascular system, but we are just beginning to understand how changes in heart and vessel structure are influenced by hemodynamic forces such as shear stress. Recent work has shown that vessel remodeling in the mouse yolk sac is secondarily effected when cardiac function is reduced or absent. These findings indicate that proper circulation is required for vessel remodeling, but have not defined whether the role of circulation is to provide mechanical cues, to deliver oxygen or to circulate signaling molecules. Here, we used time-lapse confocal microscopy to determine the role of fluid-derived forces in vessel remodeling in the developing murine yolk sac. Novel methods were used to characterize flows in normal embryos and in embryos with impaired contractility (*Mlc2a*$^{-/-}$). We found abnormal plasma and erythroblast circulation in these embryos, which led us to hypothesize that the entry of erythroblasts into circulation is a key event in triggering vessel remodeling. We tested this by sequestering erythroblasts in the blood islands, thereby lowering the hematocrit and reducing shear stress, and found that vessel remodeling and the expression of eNOS (Nos3) depends on erythroblast flow. Further, we rescued remodeling defects and eNOS expression in low-hematocrit embryos by restoring the viscosity of the blood. These data show that hemodynamic force is necessary and sufficient to induce vessel remodeling in the mammalian yolk sac.

KEY WORDS: Blood flow, Viscosity, Shear stress, Cardiovascular, Angiogenesis, eNOS (Nos3), Mlc2a (Myl7), Mouse

INTRODUCTION

The cardiovascular system is the first organ system to develop in vertebrate embryos. In the mouse, mesoderm-derived cardiac progenitors coalesce at the midline to give rise to a linear heart tube that begins to beat by early day 8 (Harvey et al., 1999; Ji et al., 2003; Tam and Schoenwolf, 1999). Concurrent with heart formation, blood and vessels first form in the extraembryonic yolk sac. By 8.5 days post-coitum (dpc), a capillary plexus consisting of a polygonal network of endothelial-lined channels is evident in the yolk sac and these vessels ultimately connect to the embryo, completing a circulatory loop between embryonic and extra-embryonic tissues. Once the heart begins to beat, primitive erythroblasts originating in the yolk sac can be found in the embryo by 4- to 6-somites (Ji et al., 2003; McGrath et al., 2003). Between 8.5 and 9.5 dpc, primitive vessels of the yolk sac undergo remodeling in the presence of flow to form a branched, hierarchical network of large and small-caliber vessels surrounded by smooth muscle cells (for a review, see Armulik et al., 2005).

The normal development of the cardiovascular system depends on a large number of genes, suggesting complex signaling pathways (Argraves and Drake, 2005; Solloway and Harvey, 2003; Trinh and Stainier, 2004). In fact, just one aspect of development – vascular remodeling in the murine yolk sac – requires over 60 known genes (our unpublished observations), including members of the Tgf-β, Notch, Vegf, hedgehog and retinoic acid signaling pathways. Although many genes required for proper vascular remodeling are expressed in endothelial cells and are thought to play a role in these cells directly, mutations in many genes required solely for cardiac function also cause defects in vascular remodeling. For instance, null mutations in *Ncx1* (also known as *Slc8a1* – Mouse Genome Informatics) (Koushik et al., 2001; Wakimoto et al., 2000), myosin light chain 2a (*Mlc2a*; also known as *Myl7* – Mouse Genome Informatics) (Huang et al., 2003), *Nkx2.5* (Tanaka et al., 1999) and titin (May et al., 2004) all exhibit failed yolk sac remodeling despite a lack of expression of these genes in endothelial cells. Furthermore, vascular abnormalities caused by the deletion of N-cadherin (cadherin 2) can be rescued by cardiac-specific expression of either N- or E-cadherin (cadherin 1) (Luo et al., 2001). To explain these effects, it has been proposed that normal blood flow is necessary for vascular remodeling. Numerous studies from avian embryos, dating back to well over a century ago, support this hypothesis because the surgical manipulation of blood flow can lead to a wide range of abnormalities in heart and vessel development (Keller, 2001; Kurz, 2000).

Whereas many studies show that blood flow is required for vessel and cardiac remodeling, what continues to be debated is the reason why blood flow is important (Conway et al., 2003; Coultas et al., 2005; Huang et al., 2003; May et al., 2004). For instance, it can be argued that blood flow is required to deliver oxygen or nutrients to remodeling tissues. Hypoxic conditions could damage endothelial cells directly or alter the levels of necessary growth factors such as Vegf (also known as Vegfa – Mouse Genome Informatics), which could impair remodeling (Conway et al., 2003; May et al., 2004). However, early mouse embryos (8.5 dpc), like early chick (Cirotto and Arangi, 1989; Pelster and Burggren, 1996; Territo and Burggren, 1998), frog (Territo and Burggren, 1998) and zebrafish embryos (Pelster and Burggren, 1996), can be cultured in the presence of carbon monoxide, which competes for oxygen binding to hemoglobin, without effecting the initial stages of vasculogenesis or vascular remodeling (E.A.V.J., S.E.F. and M.E.D., unpublished).

[1]Department of Molecular Physiology and Biophysics, Baylor College of Medicine, Houston, TX 77030, USA. [2]Department of Chemical Engineering, California Institute of Technology, Pasadena, CA 91125, USA. [3]Department of Medicine, School of Medicine, University of California-San Diego, 9500 Gilman Drive, La Jolla, CA 92093-0641, USA. [4]Biological Imaging Center, Department of Biology, California Institute of Technology, Pasadena, CA 91125, USA.

*These authors contributed equally to this work
†Author for correspondence (e-mail: mdickins@bcm.tmc.edu)

Accepted 5 July 2007

Another argument is that early blood flow functions to transport soluble nutrients, such as cell-signaling molecules that are required for vascular remodeling (Conway et al., 2003), although there is no direct evidence to support such a mechanism.

A third hypothesis for the role of circulation is that it imparts force on plexus endothelial cells and this mechanical force is necessary to activate cell-signaling cascades necessary for vessel remodeling. Blood flow exerts two types of force on vessels: shear stress, the frictional force tangential to endothelial cells, and circumferential strain, a force perpendicular to the direction of flow and which is related to intravascular pressure. Numerous studies have shown that cultured endothelial cells can respond to these forces by changing morphology, activating intracellular kinases and inducing gene expression (for a review, see Li et al., 2005) and shear stress levels in the mouse yolk sac are within the range known to induce these responses in cultured endothelial cells (Jones et al., 2004). Despite the circumstantial evidence for flow-derived force in vascular remodeling, no direct evidence exists to show that mechanical signals drive remodeling during development or to exclude the possibility that the local oxygen supply or soluble paracrine factors provided through circulation act as a trigger.

To better understand the role of circulation during early embryonic mouse development, we have used whole-embryo culture and time-lapse confocal imaging (Jones et al., 2002) to visualize and quantify blood flow in early embryos. We first used these methods to analyze dynamic events at the onset of circulation in normal mouse embryos. Next, we characterized circulation deficiencies in *Mlc2a*-null embryos to understand how secondary remodeling defects are generated by impaired cardiac contractility. Finally, we tested whether altering the mechanical properties of the early blood can phenocopy the vascular remodeling defect seen in *Mlc2a*$^{-/-}$ embryos. These studies reveal that erythroblast circulation begins after a prolonged period of plasma flow, that both plasma and erythroblast flow are disrupted in *Mlc2a* mutant embryos, and that the change in effective viscosity caused by the entry of blood cells into circulation is required to induce proper remodeling. Thus, using novel methods to analyze and manipulate blood flow in early mouse embryos, we have answered a century-old question about the role of mechanical force in vessel remodeling in vivo.

MATERIALS AND METHODS

Embryo preparation and time-lapse microscopy

Breeding pairs of *Mlc2a*$^{+/-}$*;Tg(ϵ-globin-GFP)* mice or *Tg(ϵ-globin-GFP)* mice (Dyer et al., 2001; Huang et al., 2003) were mated and the presence of a vaginal plug was taken as 0.5 dpc. Embryos were collected at 8.5 dpc and cultured for time-lapse microscopy (Jones et al., 2002). To study the initiation of flow in normal embryos, single images were taken every 6 minutes using a 20× Plan-Neofluar 0.5NA lens on a Zeiss LSM 5 PASCAL. For tracking erythroblast motion in *Mlc2a* mutants, images were taken at two frames/second using a 40× C-Apochromat 1.2NA objective. Individual cells were tracked manually by connecting the center of the same cell in subsequent images. Overlay of tracking data onto the images was performed using Adobe Photoshop.

Plasma flow measurements

To determine if plasma could be transported from the embryo to the yolk sac, 0- to 6-somite embryos were dissected as previously described (Jones et al., 2002). A pulled quartz needle (Sutter Instruments) was filled with 10×10^3 M_r fluorescein-dextran (Molecular Probes, D-1821) and a picospritzer II (General Valve Corporation) was used to inject nanoliter volumes of dye into the heart tube. Embryos were allowed to recover for up to 10 minutes at 37°C and were imaged with the Zeiss LSM PASCAL at 20× magnification to determination whether plasma was transported to the yolk sac.

For FRAP experiments, embryos at different stages were injected with 10×10^3 M_r fluorescein-dextran (50 mg/ml) and transferred to Nunc chambers (No. 155380) with culture medium (Jones et al., 2002). Embryos recovered for 15 minutes to 1 hour at 37°C. The microscope stage (Zeiss LSM 5 PASCAL or Zeiss LSM 510 META) was preheated to 37°C using a heater box (Jones et al., 2002). For reproducibility, measurements were always taken from the same region on the arterial side of the yolk sac near the caudal end of the embryo. Since the *Mlc2a* mutants cannot be unambiguously identified at the 8- to 9-somite stage, all embryos were measured blind and then genotyped after FRAP experiments. Embryos with blood cells throughout the plexus were avoided so that the movement of blood cells did not interfere with plasma measurements. For acrylamide-treated embryos (see below), acrylamide was polymerized by the addition of TEMED and embryos were allowed to recover at 37°C for 15-30 minutes prior to the injection of fluorescein-dextran (see Fig. S1 in the supplementary material). Using a 20× Plan-Apochromat 0.75 NA lens, image intensity was recorded within a region of interest (ROI) using 5% laser power. Laser power was then increased to 100% and the ROI was scanned repeatedly to bleach the fluorescence. Laser power was then reduced back to 5% to image the recovery of the dye into the bleached field. Somites were counted following the measurement.

Mean fluorescence with respect to time for the ROI was exported to a spreadsheet. The recovery curve was fitted to the equation (Soumpasis, 1983):

$$\frac{F(t)-F_0}{F_F-F_0} = e^{\frac{-2\tau}{t}}\left[I_0\left(\frac{2\tau}{t}\right)+I_1\left(\frac{2\tau}{t}\right)\right],$$

where F(t) is the fluorescence intensity, F_0 is the initial post-bleach fluorescence intensity, F_F is the final level of fluorescence recovery, I_0 and I_1 are zeroth and first order Bessel's functions, and τ is the characteristic diffusion time. The bleach area was divided by characteristic diffusion time to give the measured diffusion. The baseline for pure diffusion was obtained by injecting embryos with fluorescein-dextran as described, stopping the heart by chilling the embryos at 4°C for 1 hour, reheating the embryos to 37°C and performing FRAP.

Erythroblast immobilization

The blood islands of 5-somite stage *Tg(ϵ-globin-GFP)* embryos were gently microinjected with a 30% (w/v) solution of acrylamide:bis-acrylamide (37.5:1; 161-0158, BioRad) diluted 1:1 with 2×PBS; ammonium persulfate (161-0700, BioRad) was added to a final concentration of 10 mM (see Fig. S1 in the supplementary material). The medium was exchanged and the embryos recovered for approximately 15 minutes. To catalyze polymerization of acrylamide, TEMED (161-0801, BioRad) was diluted 1:1 with 2×PBS and applied to the blood islands using a micropipette with a low positive pressure. The tip of the micropipette was gently touched to the surface of the blood islands at a number of points to initiate gel formation. The optimal dilutions for both TEMED and acrylamide were determined by dilution series (data not shown). The medium was subsequently changed and the embryos placed in roller culture as previously described (Tam, 1998). Three sets of controls were performed: (1) uninjected embryos; (2) embryos injected only with the acrylamide solution; and (3) embryos in which only TEMED was delivered to the blood islands.

To assess embryo development, yolk sac growth and remodeling, embryos were imaged at the same magnification with a Zeiss Axiocam mounted on a Zeiss Lumar stereomicroscope equipped for fluorescence imaging. Texas Red-dextran (Molecular Probes, D-1828) was injected to better visualize remodeling. The image scale was calibrated to an etched glass standard and the yolk sac perimeter was traced using Zeiss Axiovision software. The area of the field within the traced image of the yolk sac was recorded as the size of the yolk sac. Turning was scored on a scale of 1 to 5 (1, not turned; 3, partially turned; 5, fully turned) and yolk sac vessel remodeling was scored on a scale of 1 to 5 (1, regular polygonal structure throughout yolk sac; 3, increased avascular space and lengthening of vascular segments but no obvious branching pattern; 5, hierarchical branching pattern present throughout the yolk sac with the appearance of large-caliber vessels). Embryos were not matched to their experimental group until after scoring. Statistics were performed using SPSS software

(SPSS, Chicago, IL). Data were compared using one-way ANOVA with Bonferroni post-hoc analysis. Statistical significance was determined at a level of 5% alpha error between experimental groups and control for a single measure (P<0.05).

Hetastarch injection

Hetastarch (Sigma Aldrich, H2648) consists of a high-molecular-weight hydroxyethyl starch in a physiologic saline solution (6% in 0.9% NaCl). Approximately 1-2 hours after TEMED administration, embryos received an intracardiac injection of hetastarch and were placed in roller culture.

Immunohistochemistry

Embryos were treated as described above to produce control, low-hematocrit and low-hematocrit+hetastarch groups. After 24 hours in roller culture, embryos were immediately fixed in 4% paraformaldehyde for 1 hour at 4°C then transferred to methanol or PBS for storage. Yolk sacs were incubated overnight at 4°C in one of the following primary antibodies: anti-PECAM-1 (Pinter et al., 2001), anti-VE-cadherin (R&D Systems, Minneapolis, MN; 1:100), or anti-eNOS (Santa Cruz Biotechnology, Santa Cruz, CA; 1:200). Alexa Fluor 594 or 568 secondary antibodies (Invitrogen, Carlsbad, CA) were used depending on the primary species. Images of staining patterns were collected using a Zeiss 510 META confocal system and a 40× C-Apochromat 1.2NA objective. All images for a single antibody were collected using the same laser power and detector gain settings in order to visually compare the relative intensity levels. Images shown are a maximum intensity projection of several optical slices. Each image is a representative sample of the 5-11 embryos that were stained from each group.

RESULTS

Initiation of blood flow in wild-type embryos

Previous studies showed, by examining the location of erythroblasts in fixed mouse embryos, that erythroblasts enter circulation in a stepwise pattern beginning at the 4- to 6-somite stage (Ji et al., 2003; McGrath et al., 2003). To observe the onset of circulation in live embryos, we imaged the movement of GFP-labeled erythroblasts using time-lapse confocal microscopy (Jones et al., 2002). *Tg(ϵ-globin-eGFP)* embryos (n=3) were placed in culture at the 5- to 6-somite stage (Fig. 1 and see Movie 1 in the supplementary material). During the first hour, the heart beat was evident but circulating erythroblasts were not observed (Fig. 1A,H). Occasionally, GFP+ erythroblasts were seen outside the blood islands, but only as single, adherent, stationary cells (Fig. 1A, red arrow). It is not clear whether these cells differentiated at these sites or were previously moving but had stopped. As erythroblasts begin to enter the circulation, the volume percentage of erythroblasts in vessels (hematocrit) is initially low and fluctuates from one frame to another (Fig. 1B). Many blood cells were seen to flow with a net forward motion, but some individual erythroblasts became stationary and grouped together (see Movie 1 in the supplementary material). Some groups of erythroblasts remained adherent to one another for up to 3 hours (Fig. 1, arrows) before dissociating and then rejoining the circulation. Thus, intermittent erythroblast motion was detected as early as the 6- to 7-somite stage and progressively more erythroblasts became recruited into the circulation over the next few hours.

The onset of circulation is usually defined by the movement of erythroblasts, but we were interested in determining whether significant plasma flow exists prior to erythroblast circulation. In agreement with previous findings, we detected a beating heart in embryos as early as the 3-somite stage (Navaratnam et al., 1986). To test whether the heart could pump plasma from the embryo to the yolk sac, we injected fluorescent dextran into the hearts of early-somite stage embryos and examined whether the dextran could be observed in the yolk sac plexus after a 10-minute recovery period.

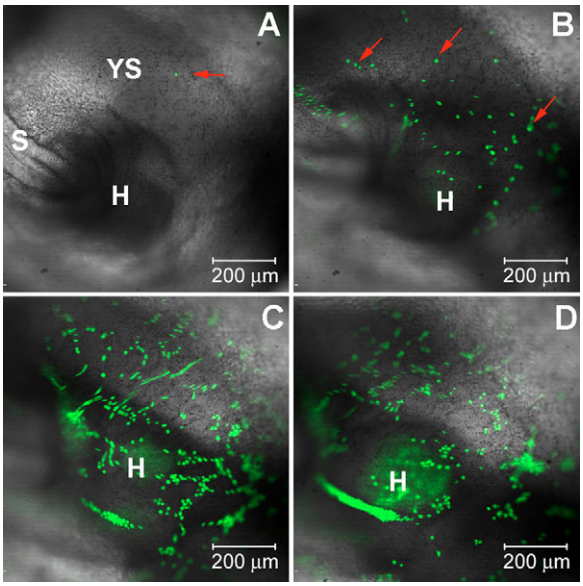

Fig. 1. Time-lapse analysis of the initiation of erythroblast circulation. Images were taken of a 6-somite mouse *Tg(ϵ-globin-GFP)* embryo every 6 minutes for a total of 12.1 hours (see Movie 1 in the supplementary material). The yolk sac (YS), heart (H) and somites (S) are indicated. (**A**) Very few erythroblasts (arrow) are visible in the yolk sac and embryo at the start of the movie (t=0). (**B**) The same field of view 1 hour later, indicating an increase in erythroblasts. Erythroblasts marked with red arrows are not circulating. (**C**) Image taken 8.1 hours after the start of the movie, showing more cells moving into the embryo and beginning to fill the heart (H). (**D**) Fluorescent cells become more evident in the heart towards the end of the time period by 11.7 hours in culture. Clumps of erythroblasts are seen as some cells stop circulating, whereas others continue to move freely.

In 0- and 1-somite stage embryos, injected dextran remained confined to the heart (n=4, data not shown). Similarly, dextran did not distribute in most 2-somite stage embryos (5 of 6 embryos, Fig. 2A,B). However, dextran was found consistently throughout the capillary plexus including the blood islands in 3-somite and older embryos (20 of 20 embryos; Fig. 2C,D). Higher magnification views of 3- and 6-somite (Fig. 2E,F) yolk sacs are shown to illustrate the distribution of the dextran within the plexus vessels. These results show that a continuous vessel network between the capillary plexus is established at least by the time the heart begins to beat.

The rapid distribution of dextran throughout the plexus suggested that there is significant plasma flow produced by the first heart beats. To confirm this, we measured plasma flow in embryos prior to the entry of erythroblasts using fluorescence recovery after photobleaching (FRAP). FRAP is used to measure the mobility of fluorescently tagged molecules by bleaching these molecules and recording how fast fluorescence intensity returns to the bleached area. The diffusion rate of 10×10^3 M_r fluorescein-dextran injected into the plexus was found to be 51±7.6 μm^2/second (n=8) in the absence of heart function (see Materials and methods). Fluorescence recovery was significantly faster than diffusion in embryos with normal circulation and we have used the term perfusion coefficient to describe these measurements of flow. At the 3- to 4-somite stage, perfusion coefficients ranged between 100 and 500 μm^2/second, indicating the presence of slow, but significant, flow (Fig. 3). The variability of plasma flow rates is not surprising given that the plexus is an extensive network of highly branched vessels with varying

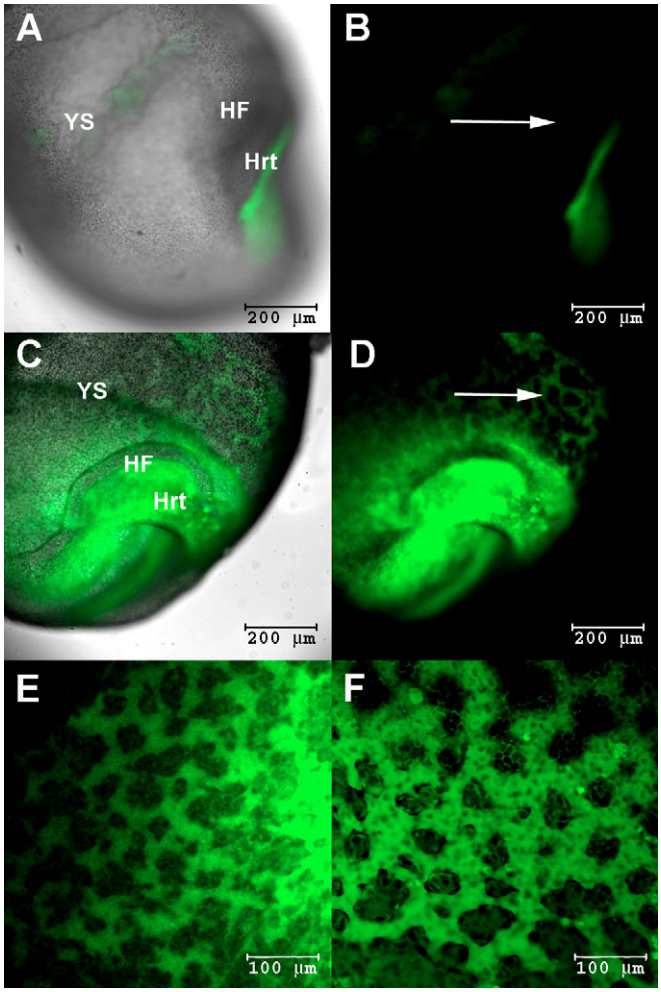

Fig. 2. Initiation of plasma flow. 10×10^3 M_r fluorescent dextran was injected into the heart (Hrt) of early mouse embryos. The embryos were incubated for 10 minutes and images were taken at 5× magnification. The presence of fluorescence in the yolk sac after such a short incubation was interpreted as the result of flowing blood plasma. In most 2-somite embryos (5 out of 6 injected embryos), dextran remains localized to the heart (**A** and **B**; arrow in B). In one case, however, fluorescent dextran could be observed throughout the yolk sac (ys) (**C** and **D**; arrow in D). Plasma circulation is consistently observed after the 3-somite stage (**E**, 3 somites; **F**, 6 somites). A and C are images taken with brightfield illumination overlaid with fluorescence images of fluorescein-dextran within the vessels (fluorescent microangiographs); B,D,E and F are microangiographs.

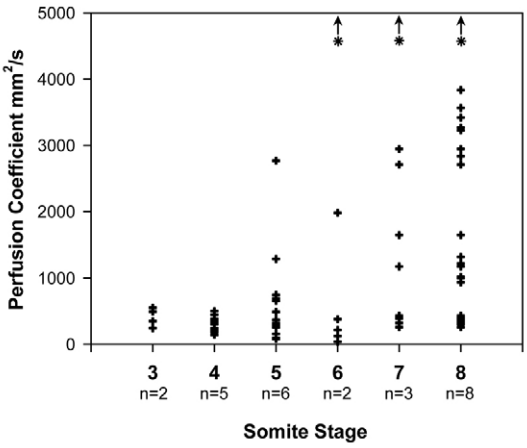

Fig. 3. Perfusion coefficients of wild-type mouse embryos. Plasma flow magnitude in the early capillary network was determined between the 3- and 8-somite stages by calculating a perfusion coefficient using FRAP. Each measurement is plotted and three measurements were made from each embryo. The total number of embryos analyzed is indicated for each stage. The upper range of perfusion coefficients increases as cardiogenesis progresses and at the 6-somite stage and later, flows that are too fast to measure are observed (asterisk and arrow). We observed a range of values even within a given embryo because flow naturally varies throughout the highly branched plexus.

resistance to flow. Perfusion values increased in later-stage embryos (5- to 6-somite stage) and plasma flow in some regions was too fast to measure (Fig. 3, indicated by asterisk with arrow). Thus, the heart is a functional pump as soon as the myocardium begins to contract and there is a significant period of plasma flow that precedes the entry of erythroblasts into circulation.

Erythroblast circulation in *Mlc2a*$^{-/-}$ embryos

Mlc2a-null mice exhibit defects in atrial contraction, ventricle filling and vascular remodeling (Huang et al., 2003), making this mutant an excellent model to study the relationship between circulation and remodeling. To visualize erythroblasts, *Mlc2a* mutant mice were crossed with *Tg(ϵ-globin-eGFP)* mice and fluorescence images of fixed *Mlc2a*$^{-/-}$*; Tg(ϵ-globin-eGFP)* embryos confirmed that vascular remodeling was impaired (Fig. 4). *Mlc2a*$^{-/-}$*; Tg(ϵ-globin-eGFP)* embryos were indistinguishable from littermates at 8.5 dpc. However, 9.5 dpc *Mlc2a*$^{-/-}$ yolk sac vessels retained the unremodeled capillary plexus, whereas *Mlc2a*$^{+/+}$ and *Mlc2a*$^{+/-}$ vessels were remodeled.

Although 8.5 dpc *Mlc2a*$^{-/-}$ embryos appear similar to littermates, we hypothesized that altered flow patterns at 8.5 dpc could be responsible for the lack of remodeling observed at 9.5 dpc. To determine whether circulation is delayed in *Mlc2a*$^{-/-}$ embryos, we compared the distribution of erythroblasts in *Mlc2a* mutant yolk sacs with heterozygote or wild-type embryos (Table 1). By the 10-somite stage, erythroblasts were routinely found throughout the plexus in wild-type and heterozygous embryos, but were not seen consistently throughout the whole yolk sac plexus until the 12- to 13-somite stage in the *Mlc2a*$^{-/-}$ embryos. Thus, erythroblast circulation appeared to be somewhat delayed in *Mlc2a*$^{-/-}$ embryos.

Next, we used time-lapse confocal microscopy to directly observe blood cell movement in *Mlc2a*$^{-/-}$ embryos. A time-lapse sequence of the initiation of flow in *Mlc2a* embryos showed that some erythroblasts began to move, but then started to form clumps. Eventually, the yolk sac filled with erythroblasts, but these cells were not flowing freely (see Fig. S2 in the supplementary material). By the 13-somite stage, normal embryos have well-established circulation and pulsatile laminar-flow profiles are observed (Jones et al., 2004). Time-lapse sequences from 13-somite *Mlc2a*$^{-/-}$ embryos showed that forward flow of erythroblasts was impaired. Erythroblasts were either stationary (data not shown) or moving in an oscillatory pattern with an equal amount of retrograde and anterograde motion (Fig. 5 and see Movie 2 in the supplementary material). Thus, instead of the rapid, pulsatile laminar-flow patterns seen in wild-type embryos, slow oscillatory flows were observed in *Mlc2a*$^{-/-}$ embryos.

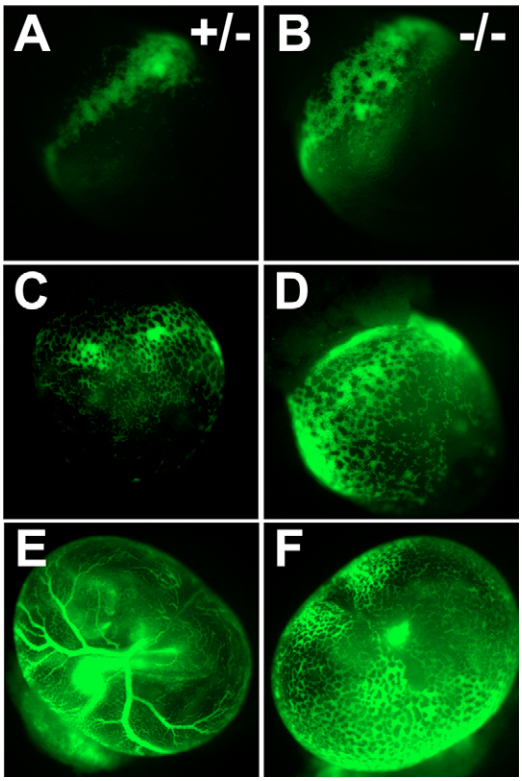

Fig. 4. Phenotype of *Mlc2a*$^{-/-}$ mouse embryos. Heterozygous (**A**,**C**,**E**) and knockout (**B**,**D**,**F**) littermates at the 7-somite (A,B), 10-somite (C,D) and 23-somite (9.5 dpc) (E,F) stage. The capillary plexus is demarcated by GFP-expressing erythroblasts. At the 7-somite stage, blood islands have clearly formed in both wild-type (A) and *Mlc2a*-null (B) embryos and erythroblasts begin to circulate in both wild-type (C) and *Mlc2a* mutant (D) embryos. However, the plexus retains an immature phenotype and fails to remodel by embryonic day 9.5 in the mutant embryos (F), as compared with wild type (E).

To determine how early the circulation is compromised, we examined plasma flow in *Mlc2a*$^{-/-}$ embryos using FRAP. Perfusion coefficients were comparable between wild-type (Fig. 3) and mutant littermates at 3- to 6-somites (data not shown), but by 8- to 9-somites, *Mlc2a*$^{-/-}$ embryos showed reduced plasma flow (Fig. 6). At 8- to 9-somites, we measured perfusion coefficients as high as 3835 μm^2/second in wild-type embryos (24 measurements in 8 embryos) and often encountered regions with flow rates too fast to measure. By contrast, perfusion coefficients in mutant embryos were nearly four-fold lower (below 1045 μm^2/second; 27 measurements in 9 embryos) and no vessels exhibited flow outside the measurable range. Of note, the perfusion coefficients measured in *Mlc2a*$^{-/-}$ embryos were still larger than pure diffusion (51±21 μm^2/second), indicating that plasma flow was present, but weaker than in wild-type embryos. These data show that poor cardiac function can be detected in very early mutant embryos, soon after the heart begins to beat and before other phenotypes are evident.

Vascular remodeling requires fluid-derived force

Data from *Mlc2a* mutants show that both plasma and erythroblast circulation are disrupted and are associated with impaired remodeling, but these experiments do not explain why flow is essential for remodeling. Since both plasma flow and erythroblast movement were impaired, it was important to establish whether proper plasma flow, which can carry soluble angiogenic factors, or the circulation of erythroblasts, which affects mechanical force and oxygen delivery, was essential. To distinguish between these possibilities, we used polymerized acrylamide to prevent erythroblasts from leaving the blood islands (see Materials and methods) to determine whether blood with a lowered hematocrit, and therefore a reduced apparent viscosity and oxygen delivery capacity, was sufficient to induce normal remodeling.

In control and untreated embryos, a hierarchical vascular branching pattern with enlarged avascular spaces was observed in yolk sacs after 24 hours in culture (Fig. 7A-C). Erythroblasts were robust in number and uniformly distributed within the vascular space (Fig. 7C). When erythroblasts were prevented from leaving the blood islands, vascular remodeling did not take place and the immature plexus persisted (Fig. 7D-F). Turning was also impaired in low-hematocrit embryos (Fig. 7D-F). To quantify these results, we established a scoring system for the extent of remodeling and turning (Table 2). These data confirm that reducing the hematocrit had a significant impact on yolk sac size, embryo turning and vessel remodeling. The methods used to reduce the hematocrit in embryos had no effect on plasma flow. Plasma flow rates were comparable to normal, untreated embryos (Fig. 8). Thus, we conclude that the circulation of plasma alone is insufficient to drive vascular remodeling, arguing against the idea that vascular remodeling is triggered by a soluble factor distributed by blood flow.

The above experiments show that erythroblast circulation is needed for remodeling. To determine if circulating erythroblasts trigger remodeling by transporting oxygen or by increasing the apparent viscosity of the circulating fluid (Chien et al., 1966), we tested whether artificially increasing the viscosity of the erythroblast-free plasma could restore remodeling. High-molecular-weight synthetic sugars derived from plants, such as hetastarch, increase the viscosity of solutions (Akers and Haidekker, 2004; Haidekker et al., 2002). We injected a hetastarch solution into the circulation of embryos with sequestered blood cells and these embryos displayed clearly visible, large, branched yolk sac vessels (Fig. 7G-I). These embryos were indistinguishable from wild type in terms of the size of the yolk sac, and the embryo turning frequency was restored (Table 2). Thus, increasing the viscosity was sufficient to rescue the remodeling deficiency in low-hematocrit embryos. We conclude that mechanical force, normally imparted by the flow of circulating erythroblasts, is necessary and sufficient to induce vessel remodeling in the yolk sac of early mouse embryos.

Expression of molecules involved in force transduction

Fluid-derived forces can directly influence cell-signaling pathways in endothelial cells (see Li et al., 2005). PECAM-1 and VE-cadherin (also known as Pecam1 and cadherin 5, respectively – Mouse Genome Informatics) are part of a complex that can act as a mechanotransducer of shear stress (Tzima et al., 2005). Also, shear stress increases the levels of the mRNA encoding nitric oxide synthase 3 (eNOS; also known as Nos3 – Mouse Genome Informatics) (Topper et al., 1996) and induces changes in the subcellular localization of eNOS protein through a PECAM-1-activated pathway (Cheng et al., 2005; Dusserre et al., 2004; Fleming et al., 2005). To determine whether these molecules play a role in force-related signaling in embryonic vessels, we examined the expression of PECAM-1, VE-cadherin and eNOS in control, low-hematocrit and low-hematocrit+hetastarch embryos. PECAM-1 (Fig. 9A-E) was observed on endothelial and erythroblast cell

Table 1. Location of erythroblasts in the vascular plexus: comparison between wild-type/heterozygous and *Mlc2a*$^{-/-}$ embryos

	Somite stage										
Location	4	5	6	7	8	9	10	11	12	13	14-15
***Mlc2a*$^{+/+}$ and *Mlc2a*$^{+/-}$**											
Blood islands (%)	67	50	37	14							
Partial plexus (%)	33	50	56	68	58	52	22				
Full plexus (%)			7	18	42	48	78	100	100	100	100
Total (*n*)	12	22	27	28	24	25	18	12	11	12	17
Mlc2a$^{-/-}$											
Blood islands (%)	86	100	33	71	14		25				
Partial plexus (%)	14		67	29	86	67	75	100			33
Full plexus (%)						33				100	66
Total (*n*)	7	4	6	7	7	6	4	4		5	3

Embryos were harvested at 8.5 dpc and were separated by somite stage. Yolk sac erythroblast location was scored as localized to the blood islands only, to the blood islands and the proximal vascular plexus, or observed throughout the blood island area and the entire vascular plexus. Shaded entries denote locations where the highest percentage of erythroblasts was observed.

membranes in both large (Fig. 9A) and small (Fig. 9B) vessels in control embryos. PECAM-1 staining appeared somewhat reduced, but was still found on the surface of endothelial cells of unremodeled vessels of the low-hematocrit yolk sacs (Fig. 9C). Since large vessels were not observed in the low-hematocrit vessels, only small vessels are shown. Robust PECAM-1 staining was observed on the endothelial cell membrane in both large (Fig. 9D) and small vessels (Fig. 9E) when plasma viscosity was restored. VE-cadherin expression was also localized to the membrane of yolk sac endothelial cells and staining appeared similar in all yolk sacs, indicating that the levels of VE-cadherin protein are not dependent on fluid force (Fig. 9F-J). In control vessels, eNOS protein was found localized to the perinuclear region as well as the cell membrane as has been described (Cheng et al., 2005). eNOS was barely detected above background in low-hematocrit embryos and localization of eNOS to membrane or perinuclear regions was not observed. eNOS expression was restored in low-hematocrit+ hetastarch embryos and membrane staining was evident on large remodeled vessels, consistent with previous findings that increased shear stress stimulates translocation of intracellular eNOS to the cell membrane (Cheng et al., 2005). Further, cell membrane proteins highlight the physical changes of endothelial cells in response to changes in mechanical force. Endothelial cells exposed to shear stress are known to elongate in the direction of the flow (Dewey et al., 1981), and elongated cells are evident in large vessels in Fig. 9. Endothelial cells in low-hematocrit vessels had a more cuboidal shape, but remained intact and retained cell-cell associations. These results show that eNOS levels are sensitive to changes in hemodynamic force during remodeling in the yolk sac and that mechanosensory signaling pathways identified in vitro also appear to regulate force responses in vivo during development

DISCUSSION

The main goal of these studies was to investigate the role of blood circulation in vessel remodeling during embryonic development. Studies of the initiation of circulation in wild-type embryos and in mutants with impaired cardiac contractility led us to hypothesize that the increase in apparent viscosity occurring when blood cells enter the circulation results in a physical stimulus that triggers remodeling. We tested this hypothesis by preventing blood cells from entering circulation, thereby reducing blood viscosity, and showed that erythroblast circulation was required for remodeling and for the proper expression of force-regulated factors. Since remodeling and the expression of force-related factors could be rescued in low-hematocrit embryos with the addition of hetastarch, we conclude that changes in the viscosity of blood, which alters the physical force exerted by the blood, are sufficient to induce vascular remodeling and to trigger signaling cascades within endothelial cells in the embryonic mouse yolk sac.

In the course of these studies, we have established a new, sensitive approach for detecting changes in early plasma circulation using FRAP. Our data show that there is plasma circulation between the

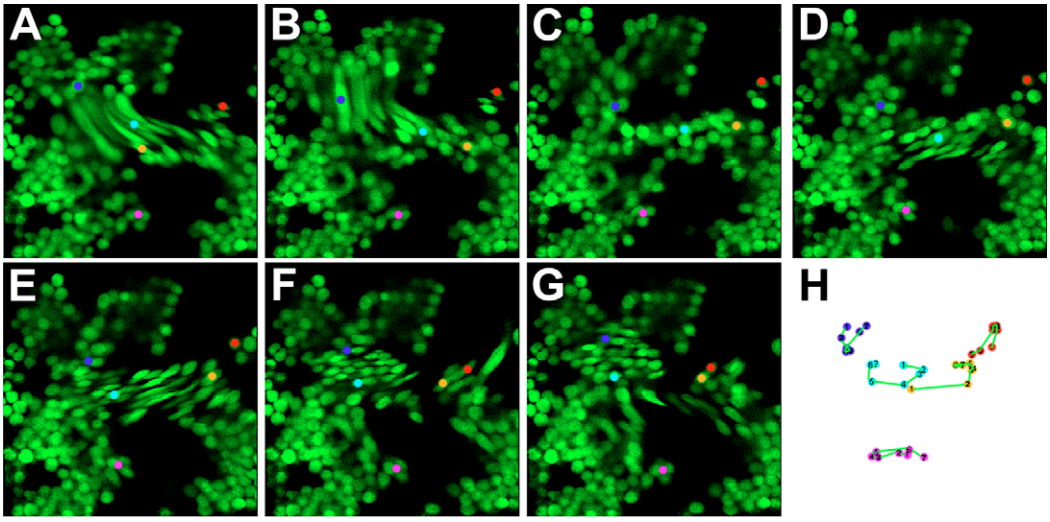

Fig. 5. Erythroblast motion in *Mlc2a*$^{-/-}$ mouse embryos. The motion of erythroblasts (green) within vessels of *Mlc2a*$^{-/-}$ embryos was imaged at two frames/second. Images were taken at (**A**) 0, (**B**) 2.5, (**C**) 5, (**D**) 7.5, (**E**) 10, (**F**) 12.5 and (**G**) 15 seconds. The motion of individual erythroblasts, marked by colored dots in A-G, were tracked and these tracks are shown (**H**), illustrating that erythroblasts oscillate with as much retrograde motion as anterograde.

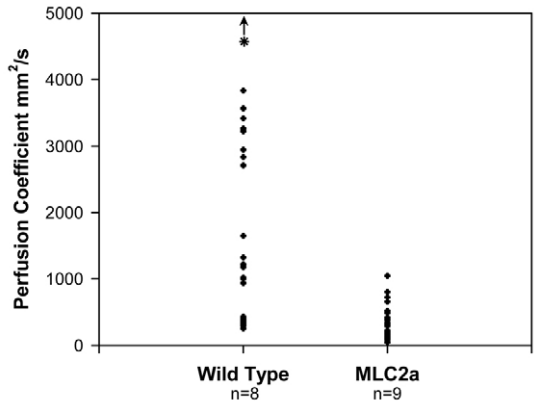

Fig. 6. Perfusion coefficients in wild-type and *Mlc2a*$^{-/-}$ mouse embryos. FRAP was used to measure perfusion coefficients within the early embryonic blood vessels in *Mlc2a*$^{-/-}$ and wild-type embryos at the 8- to 9-somite stage. Each measurement is plotted and three measurements were made from each embryo. The total number of embryos analyzed is indicated for each genotype. For reproducibility, measurements were always taken on the arterial side of the yolk sac near the caudal end of the embryo. Perfusion coefficient ranges were significantly lower in mutant than in wild-type embryos. In wild-type embryos, some perfusion coefficients were too fast to measure using FRAP (asterisk and arrow). By contrast, perfusion coefficients could always be measured in mutant embryos. Perfusion coefficients up to 3835 μm^2/second were found in wild-type embryos, whereas the maximum perfusion rate seen in *Mlc2a* mutant embryos was 1045 μm^2/second.

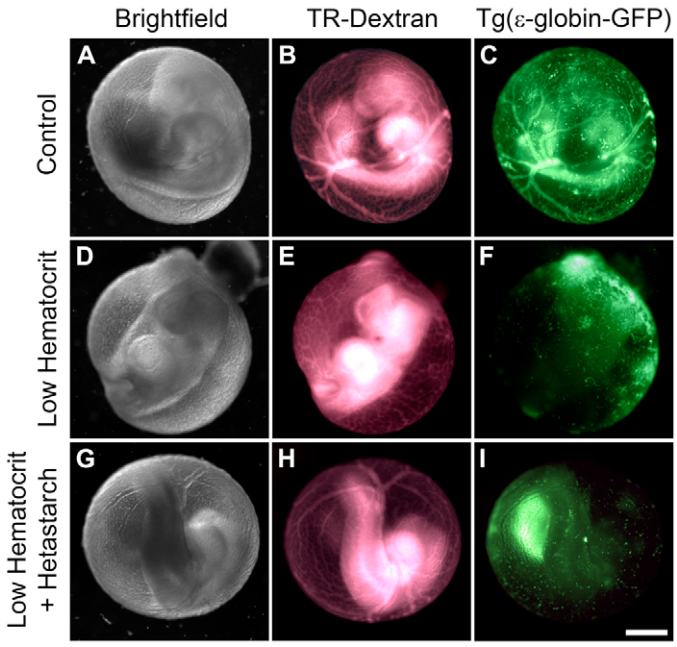

Fig. 7. Plasma viscosity alters yolk sac remodeling. Control, low-hematocrit and low-hematocrit+hetastarch mouse embryos were prepared as described (see Materials and methods). Brightfield images show that control embryos turned (**A**) and yolk sac vessels remodeled into a hierarchical, branched phenotype as evident from Texas Red (TR)-dextran microangiograms (**B**). eGFP expression (green) from the *Tg(ε-globin-GFP)* construct shows that erythroblasts are evident in all parts of the yolk sac vasculature (**C**). The embryo shown in A-C was given a score of 5 for both turning and remodeling. Embryos with sequestered erythroblasts often did not turn but continued to develop after 24 hours in culture (**D**). The yolk sac vasculature did not remodel and retained features of an immature plexus (**E**). Erythroblasts remained confined to the blood islands (**F**). This embryo was scored a 1 for both turning and remodeling. Embryo turning was restored (score=5) (**G**) and yolk sac remodeling was rescued (score=5) (**H**) in embryos with sequestered erythroblasts (**I**) after injection of the hetastarch solution. Scale bar: 500 μm.

embryo and yolk sac by the 2- to 3-somite stage, indicating that patent vessels in the yolk sac are formed by the time the heart starts to beat. This extends previous findings describing a patent heart tube by the 6-somite stage (see Ji et al., 2003). Further, defects in embryonic circulation in *Mlc2a* mutants could be detected by FRAP before an obvious phenotype was discernable and before the steady flow of erythroblasts is present. Thus, this method is effective in detecting defects in cardiac contraction prior to the onset of remodeling and can be helpful in determining whether remodeling defects are the secondary consequence of impaired heart function.

Analysis of *Mlc2a* embryos indicated that erythroblast circulation was delayed. Without the benefit of time-lapse analysis, one might conclude that there was only a minor flow abnormality, but time-lapse data revealed that flow was severely disturbed. The slow oscillatory flow in *Mlc2a* mutants is sufficient to distribute blood cells from the blood islands into more-proximal regions of the plexus, but insufficient to induce remodeling. Previous work has shown that oscillatory patterns of flow can enhance cell proliferation (Chiu et al., 1998; Davies et al., 1986; Levesque et al., 1990), but the number of proliferating cells in the yolk sac is similar in *Mlc2a* mutant and wild-type embryos (data not shown). Also, culturing mouse embryos in KB-R7943, an Ncx1 inhibitor, results in impaired remodeling, but does not induce oscillations (our unpublished data). Thus, the remodeling defect in *Mlc2a* mutant embryos is likely to be due to reduced laminar flow, rather than to the presence of abnormal oscillatory flow.

Time-lapse confocal microscopy of live embryos with GFP-labeled erythroblasts shows that erythroblasts move intermittently in the circulation by the 6- to 7-somite stage, in agreement with previous reports (Ji et al., 2003; McGrath et al., 2003; Phoon et al., 2000; Phoon et al., 2002). By physically blocking erythroblasts from leaving the blood islands, we have been able to conclude that the onset of erythroblast circulation causes a change in viscosity, which is necessary for vessel remodeling. This role for primitive erythroblasts has not yet been described because many mutations that lead to a reduction in primitive erythroblasts also affect endothelial cells directly (Oike et al., 1999; Oshima et al., 1996; Robb et al., 1995; Shalaby et al., 1995; Shivdasani et al., 1995; Suri et al., 1996; Visvader et al., 1998). It is assumed in many of these cases that disruption of the endothelial cell program is the direct cause of the remodeling defect. We would argue that any significant reduction in primitive erythroblasts alone could account for the remodeling phenotype, but presently there is no way to eliminate the erythroblast population exclusively.

In addition to affecting vessel remodeling, reducing the hematocrit also resulted in impaired embryonic turning. Although it is not entirely clear why this occurs, yolk sacs of embryos with sequestered erythroblasts are slightly smaller than control embryos (Table 2). It is possible that poor circulation reduces the tension within the yolk sac or the embryo proper leading to impaired turning. Delays in turning were also observed in *Mlc2a*-deficient embryos

Table 2. Quantitative analysis of growth, embryo turning and yolk sac vessel remodeling in control and treated embryos

Treatment	*n*	Yolk sac (mm^2)	Turn score	Remodel score
Untreated control	23	5.23±0.19	3.78±0.32	4.13±0.30
Low hematocrit	41	4.06±0.12*	1.70±0.15*	1.76±0.16*
Low hematocrit+hetastarch	19	5.19±0.28	2.68±0.32	3.58±0.30
Acrylamide only	5	4.93±0.41	3.80±0.49	4.20±0.49
TEMED only	14	5.93±0.28	4.00±0.36	4.64±0.20
Hetastarch only	12	6.05±0.24	3.50±0.44	4.25±0.37

After 24 hours in roller culture, embryos were individually imaged. The size of the yolk sac is the area of the traced image, and the embryo was assigned a score for degree of turning and degree of remodeling (see Materials and methods). A score of 1 describes an unturned embryo or unremodeled yolk sac, and a score of 5 describes a normally turned embryo and normally remodeled yolk sac.
*Significant difference ($P<0.05$) from control value.

(data not shown); however, we cannot assess whether this is a common feature of mice with hemodynamic deficiencies as it is generally not reported.

Work in both zebrafish (Isogai et al., 2003) and chick (le Noble et al., 2004) has shown that blood flow is required for the dynamic remodeling of interconnections between vessels, but is not required for vasculogenesis. Similarly, our data show that yolk sac vessels are formed and can support flow by the time the heart begins to beat, but mature vessels do not develop if viscous flow is not established. Consistent with this, endothelial cells are found lining the yolk sac plexus by the time the heart begins to beat (Ferkowicz et al., 2003; Fraser et al., 2005). Thus, it is clear that blood flow is not required for the differentiation of endothelial cells.

Our work shows that the mechanical force exerted by blood flow imparts an important signal to trigger vascular remodeling. Precisely which forces are most important for vascular remodeling remains an open question, because both shear stress and circumferential strain could be instructive. Shear stress is directly dependant on the apparent viscosity of the fluid and is likely to be the critical force acting on early endothelial cells during vascular remodeling in the mouse embryo. Shear stress has been shown to induce changes in gene expression, cytoskeletal architecture and proliferation in cultured endothelial cells (Li et al., 2005) and our previous work has shown that shear stress in early mouse circulation is well within the range known to induce these types of changes (Jones et al., 2004). Despite our evidence supporting a role for shear stress, we cannot state that shear stress is the only essential force at work in this system because circumferential strain also contributes to forces felt by endothelial cells, and we cannot distinguish a separate role for these types of forces during embryogenesis.

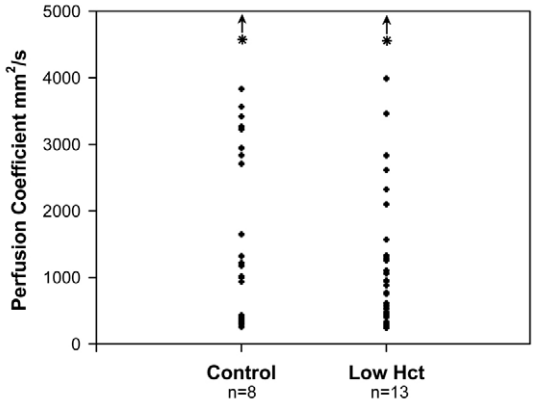

Fig. 8. Perfusion coefficients in low-hematocrit mouse embryos. To ensure that plexus plasma flow was not hampered by immobilizing the erythroblasts to the yolk sac, we determined the perfusion coefficient range in wild-type and acrylamide-treated embryos at 8- to 9-somites. Each measurement is plotted and three measurements were made from each embryo. The total number of embryos analyzed is indicated for each treatment. A similar range of measurements is seen in control and acrylamide-treated embryos indicating that plasma flow is comparable between these two groups.

Recently, there have been great strides in identifying the molecular components of a shear stress transduction pathway, implicating many molecules that are expressed during vasculogenesis and vessel remodeling (Garcia-Cardena et al., 2001; Li et al., 2005). Shear stress is thought to be sensed by a functional complex of PECAM-1, VE-cadherin and Vegfr2 (also known as Flk1 and Kdr – Mouse Genome Informatics) which, when activated, in turn activates eNOS, PI3k (Pik3r1), chicken Src and the conversion of integrins to high-affinity forms (Fleming et al., 2005; Orr et al., 2006; Topper et al., 1996; Tzima et al., 2005). Mutant analysis has gleaned only limited information about the mechanisms of force transduction in embryonic vessel remodeling. Surprisingly, PECAM-1-knockout mice on two different background strains are viable to adulthood (Duncan et al., 1999; Schenkel et al., 2006). Vegfr2 plays a role in the early differentiation of mesodermal lineages (Shalaby et al., 1997; Shalaby et al., 1995) making it difficult to assess later roles. VE-cadherin-deficient embryos fail to remodel the initial vascular plexus (Carmeliet et al., 1999; Gory-Faure et al., 1999), which would be predicted if endothelial cells could not properly sense shear stress; however, endothelial cells become detached and undergo apoptosis, which might be the primary defect (Carmeliet et al., 1999). Septal defects, deficiencies in cardiac maturation and function, vascular dysfunction, reduced angiogenesis and increased mortality are hallmarks of neonatal mice deficient in eNOS (Feng et al., 2002; Lepic et al., 2006; Zhao et al., 2002), despite the fact that these mice can survive to adulthood and reproduce. Thus, the involvement of these factors in mechanotransduction in the embryo has been difficult to define through mutant analysis. Our data show that eNOS is regulated by hemodynamic force in embryos, as would be predicted by experiments showing that mRNA levels and the subcellular localization of eNOS are regulated by shear stress in vitro (Cheng et al., 2005; Dekker et al., 2005; Dusserre et al., 2004; Fleming et al., 2005; Topper et al., 1996). Also, PECAM-1 and VE-cadherin persist on the cell surface in low-hematocrit embryos, showing that endothelial cells remain intact and continue to express molecules thought to be required for force activation. Continued expression of these proteins would be expected because low-hematocrit embryos can be rescued by restoring hemodynamic force. Overall, our data show that the mechanosensory signaling pathways identified in cultured cells also appear to be functional in vivo during development.

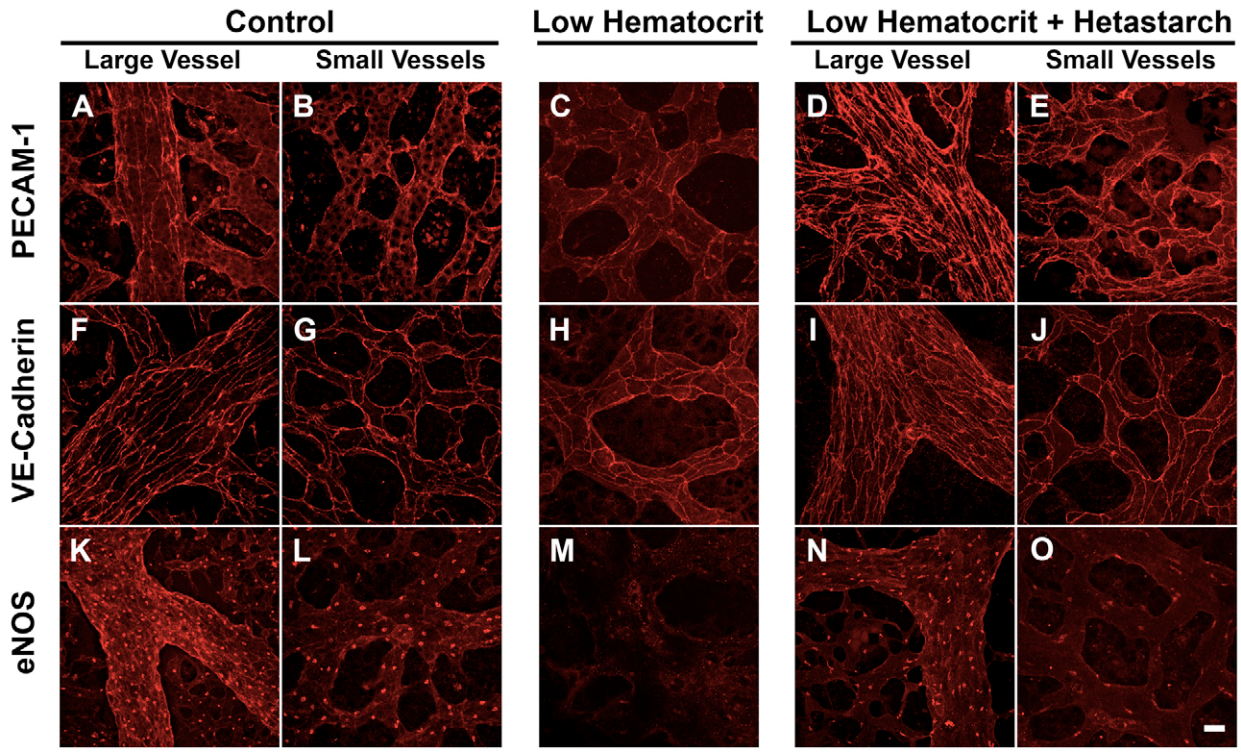

Fig. 9. Endothelial cell immunohistochemisty. Confocal images of mouse yolk sac vessels stained with PECAM-1 (**A-E**), VE-cadherin (**F-J**), and eNOS (**K-O**). A,F,K show large vessels from control yolk sacs; B,G,L are images of small vessels in controls. C,H,M are images of immunostaining in small, unremodeled vessels in low-hematocrit embryos, whereas D,I,N and E,J,O are images of large and small vessels, respectively, in low-hematocrit+hetastarch embryos. A noticeable reduction in eNOS staining was seen in low-hematocrit embryos, but both VE-cadherin and PECAM-1 staining persisted and remained localized to the plasma membrane. Elongated endothelial cell morphology in larger vessels is seen when viscous circulation is present, but unremodeled vessels had a more rounded morphology. Scale bar: 20 μm.

Conclusion

In this study, we have used novel methods to define a role for fluid-derived mechanical signaling during embryonic development. By generating methods to manipulate the physical properties of the early blood, we have been able to show that force activation of embryonic endothelial cells is required for normal vascular remodeling. Strategies such as these illustrate the strength of combining genetic and physiological methods to understand complex cardiovascular phenotypes, and open the door to further investigation of mechanical signaling in vivo.

We thank both anonymous reviewers for improving the manuscript, Margaret Baron for *Tg(ϵ-globin-GFP)* mice and for helpful discussions, Karen Hirschi and members of the Hirschi group for reading the manuscript and for helpful discussions and Josephine Enciso for the PECAM-1 antibody. This work was supported by R01 HL HL077187 (M.E.D.), a T32 HL7676 Training Grant supporting J.L.L. and an AHA Graduate Fellowship for E.A.V.J.

Supplementary material

Supplementary material for this article is available at
http://dev.biologists.org/cgi/content/full/134/18/3317/DC1

References

Akers, W. and Haidekker, M. A. (2004). A molecular rotor as viscosity sensor in aqueous colloid solutions. *J. Biomech. Eng.* **126**, 340-345.
Argraves, W. S. and Drake, C. J. (2005). Genes critical to vasculogenesis as defined by systematic analysis of vascular defects in knockout mice. *Anat. Rec. A Discov. Mol. Cell. Evol. Biol.* **286**, 875-884.
Armulik, A., Abramsson, A. and Betsholtz, C. (2005). Endothelial/pericyte interactions. *Circ. Res.* **97**, 512-523.
Carmeliet, P., Lampugnani, M. G., Moons, L., Breviario, F., Compernolle, V., Bono, F., Balconi, G., Spagnuolo, R., Oostuyse, B., Dewerchin, M. et al. (1999). Targeted deficiency or cytosolic truncation of the VE-cadherin gene in mice impairs VEGF-mediated endothelial survival and angiogenesis. *Cell* **98**, 147-157.
Cheng, C., van Haperen, R., de Waard, M., van Damme, L. C., Tempel, D., Hanemaaijer, L., van Cappellen, G. W., Bos, J., Slager, C. J., Duncker, D. J. et al. (2005). Shear stress affects the intracellular distribution of eNOS: direct demonstration by a novel in vivo technique. *Blood* **106**, 3691-3698.
Chien, S., Usami, S., Taylor, H. M., Lundberg, J. L. and Gregersen, M. I. (1966). Effects of hematocrit and plasma proteins on human blood rheology at low shear rates. *J. Appl. Physiol.* **21**, 81-87.
Chiu, J. J., Wang, D. L., Chien, S., Skalak, R. and Usami, S. (1998). Effects of disturbed flow on endothelial cells. *J. Biomech. Eng.* **120**, 2-8.
Cirotto, C. and Arangi, I. (1989). Chick embryo survival under acute carbon monoxide challenges. *Comp. Biochem. Physiol.* **94A**, 117-123.
Conway, S. J., Kruzynska-Frejtag, A., Kneer, P. L., Machnicki, M. and Koushik, S. V. (2003). What cardiovascular defect does my prenatal mouse mutant have, and why? *Genesis* **35**, 1-21.
Coultas, L., Chawengsaksophak, K. and Rossant, J. (2005). Endothelial cells and VEGF in vascular development. *Nature* **438**, 937-945.
Davies, P. F., Remuzzi, A., Gordon, E. J., Dewey, C. F., Jr and Gimbrone, M. A., Jr (1986). Turbulent fluid shear stress induces vascular endothelial cell turnover in vitro. *Proc. Natl. Acad. Sci. USA* **83**, 2114-2117.
Dekker, R. J., van Thienen, J. V., Rohlena, J., de Jager, S. C., Elderkamp, Y. W., Seppen, J., de Vries, C. J., Biessen, E. A., van Berkel, T. J., Pannekoek, H. et al. (2005). Endothelial KLF2 links local arterial shear stress levels to the expression of vascular tone-regulating genes. *Am. J. Pathol.* **167**, 609-618.
Dewey, C. F., Jr, Bussolari, S. R., Gimbrone, M. A., Jr and Davies, P. F. (1981). The dynamic response of vascular endothelial cells to fluid shear stress. *J. Biomech. Eng.* **103**, 177-185.
Duncan, G. S., Andrew, D. P., Takimoto, H., Kaufman, S. A., Yoshida, H., Spellberg, J., Luis de la Pompa, J., Elia, A., Wakeham, A., Karan-Tamir, B. et al. (1999). Genetic evidence for functional redundancy of Platelet/Endothelial cell adhesion molecule-1 (PECAM-1): CD31-deficient mice reveal PECAM-1-dependent and PECAM-1-independent functions. *J. Immunol.* **162**, 3022-3030.
Dusserre, N., L'Heureux, N., Bell, K. S., Stevens, H. Y., Yeh, J., Otte, L. A., Loufrani, L. and Frangos, J. A. (2004). PECAM-1 interacts with nitric oxide

synthase in human endothelial cells: implication for flow-induced nitric oxide synthase activation. *Arterioscler. Thromb. Vasc. Biol.* **24**, 1796-1802.
Dyer, M. A., Farrington, S. M., Mohn, D., Munday, J. R. and Baron, M. H. (2001). Indian hedgehog activates hematopoiesis and vasculogenesis and can respecify prospective neurectodermal cell fate in the mouse embryo. *Development* **128**, 1717-1730.
Feng, Q., Song, W., Lu, X., Hamilton, J. A., Lei, M., Peng, T. and Yee, S.-P. (2002). Development of heart failure and congenital septal defects in mice lacking endothelial nitric oxide synthase. *Circulation* **106**, 873-879.
Ferkowicz, M. J., Starr, M., Xie, X., Li, W., Johnson, S. A., Shelley, W. C., Morrison, P. R. and Yoder, M. C. (2003). CD41 expression defines the onset of primitive and definitive hematopoiesis in the murine embryo. *Development* **130**, 4393-4403.
Fleming, I., Fisslthaler, B., Dixit, M. and Busse, R. (2005). Role of PECAM-1 in the shear-stress-induced activation of Akt and the endothelial nitric oxide synthase (eNOS) in endothelial cells. *J. Cell Sci.* **118**, 4103-4111.
Fraser, S. T., Hadjantonakis, A. K., Sahr, K. E., Willey, S., Kelly, O. G., Jones, E. A., Dickinson, M. E. and Baron, M. H. (2005). Using a histone yellow fluorescent protein fusion for tagging and tracking endothelial cells in ES cells and mice. *Genesis* **42**, 162-171.
Garcia-Cardena, G., Comander, J., Anderson, K. R., Blackman, B. R. and Gimbrone, M. A., Jr (2001). Biomechanical activation of vascular endothelium as a determinant of its functional phenotype. *Proc. Natl. Acad. Sci. USA* **98**, 4478-4485.
Gory-Faure, S., Prandini, M. H., Pointu, H., Roullot, V., Pignot-Paintrand, I., Vernet, M. and Huber, P. (1999). Role of vascular endothelial-cadherin in vascular morphogenesis. *Development* **126**, 2093-2102.
Haidekker, M. A., Tsai, A. G., Brady, T., Stevens, H. Y., Frangos, J. A., Theodorakis, E. and Intaglietta, M. (2002). A novel approach to blood plasma viscosity measurement using fluorescent molecular rotors. *Am. J. Physiol.* **282**, H1609-H1614.
Harvey, R. P., Biben, C. and Elliott, D. A. (1999). Transcriptional control and pattern formation in the developing vertebrate heart: studies on NK-2 class homeodomain factors. In *Heart Development* (ed. R. P. Harvey and N. Rosenthal), pp. 111-129. San Diego: Academic Press.
Huang, C., Sheikh, F., Hollander, M., Cai, C., Becker, D., Chu, P. H., Evans, S. and Chen, J. (2003). Embryonic atrial function is essential for mouse embryogenesis, cardiac morphogenesis and angiogenesis. *Development* **130**, 6111-6119.
Isogai, S., Lawson, N. D., Torrealday, S., Horiguchi, M. and Weinstein, B. M. (2003). Angiogenic network formation in the developing vertebrate trunk. *Development* **130**, 5281-5290.
Ji, R. P., Phoon, C. K., Aristizabal, O., McGrath, K. E., Palis, J. and Turnbull, D. H. (2003). Onset of cardiac function during early mouse embryogenesis coincides with entry of primitive erythroblasts into the embryo proper. *Circ. Res.* **92**, 133-135.
Jones, E. A., Crotty, D., Kulesa, P. M., Waters, C. W., Baron, M. H., Fraser, S. E. and Dickinson, M. E. (2002). Dynamic in vivo imaging of postimplantation mammalian embryos using whole embryo culture. *Genesis* **34**, 228-235.
Jones, E. A., Baron, M. H., Fraser, S. E. and Dickinson, M. E. (2004). Measuring hemodynamic changes during mammalian development. *Am. J. Physiol.* **287**, H1561-H1569.
Keller, B. B. (2001). Function and biomechanics of developing cardiovascular systems. In *Formation of the Heart and its Regulation* (ed. R. J. Tomanek and R. B. Runyan), pp. 251-271. New York: Springer Verlag.
Koushik, S. V., Wang, J., Rogers, R., Moskophidis, D., Lambert, N. A., Creazzo, T. L. and Conway, S. J. (2001). Targeted inactivation of the sodium-calcium exchanger (Ncx1) results in the lack of a heartbeat and abnormal myofibrillar organization. *FASEB J.* **15**, 1209-1211.
Kurz, H. (2000). Physiology of angiogenesis. *J. Neurooncol.* **50**, 17-35.
le Noble, F., Moyon, D., Pardanaud, L., Yuan, L., Djonov, V., Matthijsen, R., Breant, C., Fleury, V. and Eichmann, A. (2004). Flow regulates arterial-venous differentiation in the chick embryo yolk sac. *Development* **131**, 361-375.
Lepic, E., Burger, D., Lu, X., Song, W. and Feng, Q. (2006). Lack of endothelial nitric oxide synthase decreases cardiomyocyte proliferation and delays cardiac maturation. *Am. J. Physiol.* **291**, C1240-C1246.
Levesque, M. J., Nerem, R. M. and Sprague, E. A. (1990). Vascular endothelial cell proliferation in culture and the influence of flow. *Biomaterials* **11**, 702-707.
Li, Y. S., Haga, J. H. and Chien, S. (2005). Molecular basis of the effects of shear stress on vascular endothelial cells. *J. Biomech.* **38**, 1949-1971.
Luo, Y., Ferreira-Cornwell, M., Baldwin, H., Kostetskii, I., Lenox, J., Lieberman, M. and Radice, G. (2001). Rescuing the N-cadherin knockout by cardiac-specific expression of N- or E-cadherin. *Development* **128**, 459-469.
May, S. R., Stewart, N. J., Chang, W. and Peterson, A. S. (2004). A Titin mutation defines roles for circulation in endothelial morphogenesis. *Dev. Biol.* **270**, 31-46.
McGrath, K. E., Koniski, A. D., Malik, J. and Palis, J. (2003). Circulation is established in a stepwise pattern in the mammalian embryo. *Blood* **101**, 1669-1676.
Navaratnam, V., Kaufman, M. H., Skepper, J. N., Barton, S. and Guttridge, K. M. (1986). Differentiation of the myocardial rudiment of mouse embryos: an ultrastructural study including freeze-fracture replication. *J. Anat.* **146**, 65-85.
Oike, Y., Takakura, N., Hata, A., Kaname, T., Akizuki, M., Yamaguchi, Y., Yasue, H., Araki, K., Yamamura, K. and Suda, T. (1999). Mice homozygous for a truncated form of CREB-binding protein exhibit defects in hematopoiesis and vasculo-angiogenesis. *Blood* **93**, 2771-2779.
Orr, A. W., Helmke, B. P., Blackman, B. R. and Schwartz, M. A. (2006). Mechanisms of mechanotransduction. *Dev. Cell* **10**, 11-20.
Oshima, M., Oshima, H. and Taketo, M. M. (1996). TGF-beta receptor type II deficiency results in defects of yolk sac hematopoiesis and vasculogenesis. *Dev. Biol.* **179**, 297-302.
Pelster, B. and Burggren, W. W. (1996). Disruption of hemoglobin oxygen transport does not impact oxygen- dependent physiological processes in developing embryos of zebra fish (Danio rerio). *Circ. Res.* **79**, 358-362.
Phoon, C. K., Aristizabal, O. and Turnbull, D. H. (2000). 40 MHz Doppler characterization of umbilical and dorsal aortic blood flow in the early mouse embryo. *Ultrasound Med. Biol.* **26**, 1275-1283.
Phoon, C. K., Aristizabal, O. and Turnbull, D. H. (2002). Spatial velocity profile in mouse embryonic aorta and Doppler-derived volumetric flow: a preliminary model. *Am. J. Physiol.* **283**, H908-H916.
Pinter, E., Haigh, J., Nagy, A. and Madri, J. A. (2001). Hyperglycemia-induced vasculopathy in the murine conceptus is mediated via reductions of VEGF-A expression and VEGF receptor activation. *Am. J. Pathol.* **158**, 1199-1206.
Robb, L., Lyons, I., Li, R., Hartley, L., Kontgen, F., Harvey, R. P., Metcalf, D. and Begley, C. G. (1995). Absence of yolk sac hematopoiesis from mice with a targeted disruption of the scl gene. *Proc. Natl. Acad. Sci. USA* **92**, 7075-7079.
Schenkel, A. R., Chew, T. W., Chlipala, E., Harbord, M. W. N. and Muller, W. A. (2006). Different susceptibilities of PECAM-deficient mouse strains to spontaneous idiopathic pneumonitis. *Exp. Mol. Pathol.* **81**, 23.
Shalaby, F., Rossant, J., Yamaguchi, T. P., Gertsenstein, M., Wu, X. F., Breitman, M. L. and Schuh, A. C. (1995). Failure of blood-island formation and vasculogenesis in Flk-1-deficient mice. *Nature* **376**, 62-66.
Shalaby, F., Ho, J., Stanford, W. L., Fischer, K. D., Schuh, A. C., Schwartz, L., Bernstein, A. and Rossant, J. (1997). A requirement for Flk1 in primitive and definitive hematopoiesis and vasculogenesis. *Cell* **89**, 981-990.
Shivdasani, R. A., Mayer, E. L. and Orkin, S. H. (1995). Absence of blood formation in mice lacking the T-cell leukaemia oncoprotein tal-1/SCL. *Nature* **373**, 432-434.
Solloway, M. J. and Harvey, R. P. (2003). Molecular pathways in myocardial development: a stem cell perspective. *Cardiovasc. Res.* **58**, 264-277.
Soumpasis, D. M. (1983). Theoretical analysis of fluorescence photobleaching recovery experiments. *Biophys. J.* **41**, 95-97.
Suri, C., Jones, P. F., Patan, S., Bartunkova, S., Maisonpierre, P. C., Davis, S., Sato, T. N. and Yancopoulos, G. D. (1996). Requisite role of angiopoietin-1, a ligand for the TIE2 receptor, during embryonic angiogenesis. *Cell* **87**, 1171-1180.
Tam, P. P. (1998). Postimplantation mouse development: whole embryo culture and micro- manipulation. *Int. J. Dev. Biol.* **42**, 895-902.
Tam, P. P. L. and Schoenwolf, G. C. (1999). Cardiac fate maps: lineage allocation, morphogenetic movement, and cell commitment. In *Heart Development* (ed. R. P. Harvey and N. Rosenthal), pp. 3-17. San Diego: Academic Press.
Tanaka, M., Chen, Z., Bartunkova, S., Yamasaki, N. and Izumo, S. (1999). The cardiac homeobox gene Csx/Nkx2.5 lies genetically upstream of multiple genes essential for heart development. *Development* **126**, 1269-1280.
Territo, P. R. and Burggren, W. W. (1998). Cardio-respiratory ontogeny during chronic carbon monoxide exposure in the clawed frog Xenopus laevis. *J. Exp. Biol.* **201**, 1461-1472.
Topper, J. N., Cai, J., Falb, D. and Gimbrone, M. A., Jr (1996). Identification of vascular endothelial genes differentially responsive to fluid mechanical stimuli: cyclooxygenase-2, manganese superoxide dismutase, and endothelial cell nitric oxide synthase are selectively up-regulated by steady laminar shear stress. *Proc. Natl. Acad. Sci. USA* **93**, 10417-10422.
Trinh, L. A. and Stainier, D. Y. (2004). Cardiac development. *Methods Cell Biol.* **76**, 455-473.
Tzima, E., Irani-Tehrani, M., Kiosses, W. B., Dejana, E., Schultz, D. A., Engelhardt, B., Cao, G., DeLisser, H. and Schwartz, M. A. (2005). A mechanosensory complex that mediates the endothelial cell response to fluid shear stress. *Nature* **437**, 426-431.
Visvader, J. E., Fujiwara, Y. and Orkin, S. H. (1998). Unsuspected role for the T-cell leukemia protein SCL/tal-1 in vascular development. *Genes Dev.* **12**, 473-479.
Wakimoto, K., Kobayashi, K., Kuro, O. M., Yao, A., Iwamoto, T., Yanaka, N., Kita, S., Nishida, A., Azuma, S., Toyoda, Y. et al. (2000). Targeted disruption of Na+/Ca2+ exchanger gene leads to cardiomyocyte apoptosis and defects in heartbeat. *J. Biol. Chem.* **275**, 36991-36998.
Zhao, X., Lu, X. and Feng, Q. (2002). Deficiency in endothelial nitric oxide synthase impairs myocardial angiogenesis. *Am. J. Physiol.* **283**, H2371-H2378.